

On the Impact of Neutron Star Binaries Natal-Kick Distribution on the Galactic r-process Enrichment

Mohammadtaher Safarzadeh^{1*}, Benoit Côté^{2,3,4}

¹*School of Earth and Space Exploration, Arizona State University, Tempe, AZ 85287-1404, USA;*

²*Department of Physics and Astronomy, University of Victoria, Victoria, BC, V8W 2Y2, Canada;*

³*National Superconducting Cyclotron Laboratory, Michigan State University, East Lansing, MI, 48824, USA;*

⁴*Joint Institute for Nuclear Astrophysics - Center for the Evolution of the Elements, USA*

13 November 2021

ABSTRACT

We study the impact of the neutron star binaries' (NSBs) natal kick distribution on the Galactic r-process enrichment. We model the growth of a Milky Way type halo based on N-body simulation results and its star formation history based on multi epoch abundance matching techniques. We consider the NSBs that merge well beyond the galaxy's effective radius ($> 2 \times R_{\text{eff}}$) do not contribute to Galactic r-process enrichment. Assuming a power-law delay-time distribution (DTD) function ($\propto t^{-1}$) with $t_{\text{min}} = 30$ Myr for binaries' coalescence timescales, and an exponential profile for their natal kick distribution with an average value of 180 km s^{-1} , we show that up to $\sim 40\%$ of all formed NSBs do not contribute to r-process enrichment by $z = 0$, either because they merge far from the galaxy at a given redshift (up to $\sim 25\%$) or have not yet merged by today ($\sim 15\%$). Our result is largely insensitive to the details of the DTD function. Assuming a constant coalescence timescale of 100 Myr well approximates the adopted DTD with 30% of the NSBs not contributing to r-process enrichment. Our results, although rather dependent on the adopted natal kick distribution, represent a first step towards estimating the impact of natal kicks and DTD functions on r-process enrichment of galaxies that would need to be incorporated in the hydrodynamical simulations.

Key words: Galaxy: abundances – stars: neutron – stars: natal kicks

1 INTRODUCTION

Neutron star mergers (NSMs) and core collapse supernovae (SNcc) are the two main candidates to explain the observed Galactic r-process enrichment (Cowan et al. 1991; Woosley et al. 1994; Rosswog et al. 1999, 2000; Argast et al. 2004). Though the rate of NSMs is orders of magnitude less than SNcc, they have orders of magnitude higher r-process yields. Although heavy r-process elements could be produced under extreme conditions of a magnetorotational core-collapse supernovae (Winteler et al. 2012; Nishimura et al. 2015), recent hydrodynamical simulations of core-collapse supernovae with detailed treatment of neutrino transport show that it is highly difficult to synthesize r-process elements heavier than $A > 110$ (Wanajo et al. 2010; Martínez-Pinedo et al. 2012; Roberts et al. 2012; Fischer et al. 2012; Wanajo 2013). This leaves NSMs as potentially the only robust source of heavy r-process elements (Wanajo et al. 2014; Goriely et al. 2015).

Hydrodynamical simulations have been successful at re-

producing the observed abundance of r-process elements by assuming NSMs as the only source of r-process elements in the Galaxy (van de Voort et al. 2015; Shen et al. 2015). Hirai et al. (2015) demonstrated that, even with a delay time of 100 Myr, NSM ejecta can still enrich low-metallicity stars when reducing the star formation efficiency of low-mass building block galaxies. This conclusion was also predicted by the simple model of Ishimaru et al. (2015) and the semi-analytic model of Komiya & Shigeyama (2016). We refer to Côté et al. (2017) for a review of recent r-process enrichment studies for the MW.

There are two main sources of uncertainty when modeling NSMs as sources of r-process enrichment in the Galaxy. The NSM rate, which can vary by 2 or 3 orders of magnitudes according to population synthesis models (Dominik et al. 2012), and r-process ejected mass in a NSM event with a wide range from $10^{-4} - 4 \times 10^{-2} M_{\odot}$ (Oechslin et al. 2002; Goriely et al. 2011; Korobkin et al. 2012; Piran et al. 2013). The escape of NSBs from the host halo due to the natal kicks is the third uncertain factor when modeling r-process enrichment with NSMs. Depending on the merging

* E-mail: mts@asu.edu

time scale associated to them and the host halo mass they reside in, NSBs can merge well beyond their host galaxy (Bloom et al. 1999; Fryer et al. 1999; Belczynski et al. 2006; Zemp et al. 2009; Kelley et al. 2010; Behroozi et al. 2014) and therefore be regarded as host-less merging events which do not contribute to r-process enrichment.

The impact of natal kicks has been studied before in different contexts mainly related to short gamma-ray burst (sGRBs). Behroozi et al. (2014) studied the impact of natal kicks on the fraction of host-less sGRBs (Berger 2010) from N-Body simulations and merger tree studies. Kelley et al. (2010) studied this in the context of spatial distribution of sGRBs on the sky and the predictions for future gravitational wave experiments. Bramante & Linden (2016) considered the natal kick impact on r-process enrichment of ultra faint dwarf galaxies (UFDs, Brown et al. 2012; Frebel & Bromm 2012; Vargas et al. 2013) and concluded that natal kicks most certainly remove the NS binary from the UFD progenitor at redshifts of reionization and suggested alternative pathways to explode a lone NS. Unless very short timescales for merging of a NS binary is possible due to Kozai effect (Shappee & Thompson 2013; Beniamini et al. 2016) or a common envelope scenario (Belczynski et al. 2002), the NS binary will tend to travel away from the host and therefore not contribute to r-process enrichment.

Here we investigate how such considerations would affect the results of r-process enrichment codes. We follow the MW progenitor halo growth history modeled analytically based on Bolshoi N-Body simulations merger trees. Given a parametrized star formation history (SFH) for a MW type halo at $z = 0$ based on multi epoch abundance matching techniques, we compute the fraction of NSBs that would merge within a multiple of their host galaxy's effective radius given a natal kick velocity probability distribution function (PDF) and a delay-time distribution assigned to the NSBs.

In §2 we describe our method in more detail. In §3 we present our results. In §4 we present a discussion of our results and in §5 we give conclusions.

2 METHOD

In this section, we describe how we model the evolution of the dark matter halo and its central galaxy as a function of redshift. We then describe the formation and the trajectory calculation of NSBs in order to predict what fraction of them do not contribute to the galactic r-process enrichment.

2.1 Evolution of the Dark Matter Halo

We consider a MW-like dark matter halo with a current mass of $10^{12} M_{\odot}$ (Wang et al. 2015). We use the relations derived by Behroozi et al. (2013) from the *Bolshoi* simulation (Klypin et al. 2011) to calculate the evolution of the dark matter mass M_{DM} as a function of redshift (z). We express the halo radius (R_{200}) defined as enclosing overdensity of 200 times the critical density of the universe at a given redshift, $\rho_{\text{cr}}(z)$, so $M_{200} = (4\pi/3)200\rho_{\text{cr}}(z)R_{200}^3$. With this setup, $R_{200} = 209$ kpc at $z = 0$. Values for the cosmological parameters are taken from Planck Collaboration et al. (2016): $H_0 = 100h$ km s $^{-1}$ Mpc $^{-1}$, $h = 0.678$, $\Omega_0 = 0.308$, $\Omega_{\Lambda,0} = 0.692$.

2.2 Dark Matter Gravitational Potential

At each redshift, the radial gravitational potential profile of the NFW dark matter halo is

$$\Phi(r) = -\frac{GM_{\text{DM}}\ln(1 + c_{200}r/R_{200})}{[\ln(1 + c_{200}) - c_{200}/(1 + c_{200})]r}, \quad (1)$$

where G is the Newton gravitational constant and c_{200} is the concentration parameter of the dark matter halo we assign following Dutton & Macciò (2014). The acceleration g acting on a NS binary as a function of radius is given by the derivative of the potential profile,

$$g(r) = \frac{d\Phi}{dr} = A_{\Phi} \left(\frac{\beta}{r(1 + \beta r)} - \frac{\ln(1 + \beta r)}{r^2} \right), \quad (2)$$

$$\beta \equiv c_{200}/R_{200}, \quad (3)$$

$$A_{\Phi} = -\frac{GM_{\text{DM}}}{\ln(1 + c_{200}) - c_{200}/(1 + c_{200})}. \quad (4)$$

In these last equations, M_{DM} , R_{200} , and c_{200} are constant with radius, but are still dependent on redshift.

2.3 Evolution of the Central Galaxy

We describe the central galaxy by its effective radius and its stellar mass content. For star formation history of a MW type halo, we adopt the parametrization presented in Moster et al. (2013) which is based on a multi epoch abundance matching technique. From this relation, we create several redshift bins with constant redshift intervals, convert redshifts into times, and integrate the star formation history to recover the total stellar mass of the galaxy for each redshift bin. In our model, at $z = 0$, the star formation rate is $2.63 M_{\odot} \text{ yr}^{-1}$ and the total integrated stellar mass is $5.43 \times 10^{10} M_{\odot}$.

We set the effective radius R_{eff} of the galaxy to a fraction of the virial radius of its host dark matter halo (Kravtsov 2013),

$$R_{\text{eff}}(z) \equiv 0.032R_{200}(z). \quad (5)$$

The proportionality constant has been tuned to reproduce the observed relation derived by van der Wel et al. (2014) between R_{eff} , redshift, and the stellar mass of late-type blue galaxies up to $z = 3$. This value is about twice the value derived by Kravtsov (2013) but is still within the observational scatter (see their Figure 1). At $z = 0$, Equation 5 yields $R_{\text{eff}} \approx 6.7$ kpc.

2.4 Neutron Star Binaries

In this work, we assume that 2×10^{-5} NSB system will lead to a NSM per units of stellar mass formed, a number adopted in the chemical evolution study of Côté et al. (2017). The input number of NSMs is typically calibrated to reproduce the current Galactic NSM rate estimated by binary pulsars (Kalogera et al. 2004; Abadie et al. 2010), as in the chemical evolution studies of Matteucci et al. (2014), Cescutti et al.

(2015), Hirai et al. (2015), van de Voort et al. (2015), and Wehmeyer et al. (2015). This number can also be extracted from population synthesis predictions (Dominik et al. 2012), as in Ishimaru et al. (2015), or derived from NSM yields and observed chemical abundances (Shen et al. 2015). In our study, however, the total number of NSMs is only relevant for the statistics of our Monte Carlo calculations and does not have an impact on our conclusions (see Section 4).

Each NS is expected to receive a natal kick that can reach several hundreds of km s^{-1} . Different probability distributions as been proposed to explain the observed NS velocities such as a single Maxwellian distribution (e.g., Hansen & Phinney 1997; Hobbs et al. 2005) and a bimodal distribution (e.g., Fryer et al. 1998; Arzoumanian et al. 2002). However, the final velocity kick imparted to a NSB system is more complicated, as the system experiences two different kicks and the orbital properties of the binary must be taken into account (Fryer et al. 1998). Belczynski et al. (2002) showed that the velocity of a NSB significantly changes after the second kick generated by the second supernova explosion. In addition, a too large velocity kick imparted to a NS can unbound or significantly increase the coalescence timescale of NSBs. (Belczynski & Bulik 1999; Kalogera & Lorimer 2000).

We assign a unique initial natal kick velocity v_{kick} to each NSB by randomly sampling an exponential probability distribution function (PDF) defined as (Behroozi et al. 2014)

$$\text{PDF}(v_{\text{kick}}) = \exp\left(-\frac{v_{\text{kick}}}{\langle v \rangle}\right), \quad (6)$$

where $\langle v \rangle$ represents the average natal kick velocity, which is set to 180 km s^{-1} . This PDF has been derived to approximate the NS binary natal kick distribution predicted by the population synthesis model of Fryer et al. (1998), which uses a bimodal kick distribution for each individual NS.

Once a kick is sampled, a unique NSM coalescence time t_{coal} is assigned to each NSB by randomly sampling a power-law delay-time distribution (DTD) function defined as (e.g., Dominik et al. 2012)

$$\text{PDF}(t_{\text{coal}}) = t_{\text{coal}}^{-1}. \quad (7)$$

For our fiducial case, we assume that the minimum and maximum coalescence times are 30 Myr and 10 Gyr, respectively. The minimum time is motivated by the standard population synthesis models of Belczynski et al. (2016) (see Figure 8 in Côté et al. 2017). We note that some NSBs can have a coalescence time larger than the Hubble time (Lorimer 2008). However, because of the functional form of the adopted DTD, extending the maximum coalescence time beyond 10 Gyr will have negligible impact on our results.

To perform our Monte Carlo simulation in a consistent manner, we restructure the redshift bins to ensure to form the same number (here 1000) of NSM candidate binaries in each bin. Otherwise, the scatter in the results would vary as a function of redshift, which would be a numerical artifact. In Section 3, we compare our results with constant coalescence timescales of 30 and 100 Myr to connect with some galactic *r*-process enrichment studies (e.g., Matteucci et al. 2014; Cescutti et al. 2015; Wehmeyer et al. 2015; Côté et al. 2017; Hirai et al. 2017).

All PDFs are assumed to be similar at all redshifts. This is a first order approximation, since according to population

synthesis models, the number and DTD function of NSMs should vary with metallicity and therefore with redshift (e.g., Dominik et al. 2012; Belczynski et al. 2016).

2.5 Non-Contributing Neutron Star Binaries

Here we describe our procedure to calculate the fraction of NSBs that do not contribute to *r*-process enrichment, either because they merge beyond the galaxy or because they do not have time to merge by $z = 0$. Throughout this paper, all of our NSBs have a coalescence time shorter than 10 Gyr (see Section 2.4).

For each redshift bin, starting at the highest redshift, we define an enclosing radius R_{enc} based on the effective radius of the galaxy,

$$R_{\text{enc}} \equiv f_{\text{enc}} R_{\text{eff}}. \quad (8)$$

All NSMs that occur above this threshold radius are assumed to not contribute to *r*-process enrichment of the galaxy. NSM ejecta have very large speeds around $v_{\text{ejc}} \sim 0.2c$ with a stopping length of $l_s \sim (2.6/n_{\text{H}}) \text{ kpc}$ where n_{H} is the number density of the Hydrogen atom in cm^{-3} in which the NSM goes off (Komiya & Shigeyama 2016). If the NSM event occurs outside the enclosing radius that we consider in this paper, the medium has densities of $n_{\text{H}} \ll 0.1 \text{ cm}^{-3}$, which means $l_s \gg 30 \text{ kpc}$. Such large stopping length translates into a very diluted gas in *r*-process elements. Stars forming out of such diluted gas will show no detectable *r*-process enhancement, and even if this gas falls back into the ISM of the host galaxy, its contribution to *r*-process enrichment compared to the gas that is enriched with a NSM going off inside the enclosing radius is deemed negligible.

In Section 3, we test $f_{\text{enc}} = 2$ and 4 with a fiducial value of 2. Although we assume that all NSBs originate from the center of the host dark matter halo, we do not explore values lower than $f_{\text{enc}} = 2$ because it represents the minimum length to cross the galaxy's effective volume from one side to the other. In our calculation, we do not account for a stellar disc geometry and potential.

For each NSB, we randomly sample v_{kick} and t_{coal} and calculate the trajectory of the binary system by integrating the classical equations of motion. With an initial velocity of v_{kick} , we follow the trajectories until t_{coal} using the radius-dependent gravitational acceleration defined in Equation 2, which also depends on the characteristics of the dark matter halo (see Section 2.1). We assume that the radial gravitational potential profile does not change through a trajectory calculation.

Depending on v_{kick} , t_{coal} , and the gravitational potential, the trajectory can be oscillating around the galaxy center. After a time t_{coal} , we compare the final radius with R_{enc} (Equation 8) and define whether or not the NSB will contribute to the galactic enrichment of *r*-process elements. If the radius becomes larger than R_{200} during the calculation, we stop to follow the trajectory and assume that the NSB do not contribute to *r*-process enrichment.

3 RESULTS

Figure 1 shows our main results for a MW type halo where we have tracked the NSBs trajectory inside their host virial-

ized halo. The blue dashed line shows the median of 100 realizations of our simulations for the fraction of NSBs formed at a given redshift z that merge beyond the Galaxy’s effective radius and therefore considered as not contributing to r-process enrichment of the halo at $z = 0$. The green dashed line shows NSBs formed at $z = z$ and have not yet merged by $z = 0$ because of their delayed coalescence timescale. As the potential well of the host halo becomes deeper with time, the fraction of NSBs that merge outside the Galaxy and do not contribute to r-process enrichment drops with time from $\sim 60\%$ at $z = 5$ to almost zero percent at $z = 0$. We have assumed a delay-time distribution in the form of a power law from $t_{\min} = 30$ Myr to $t_{\max} = 10$ Gyr for our fiducial analysis. At redshifts lower than $z \sim 2$ the NSBs start to not contribute to r-process enrichment because of the delay they experience before merging (green dashed line). This fact will increase the total fraction of the NSBs that eventually not contribute to r-process enrichment of the Galaxy at $z = 0$.

The cumulative picture of the results described above is shown with solid lines in Figure 1. The solid blue line shows the cumulative fraction of the NSBs that never contribute to r-process enrichment by $z = z$ due to merging beyond R_{enc} while the solid green line shows the cumulative fraction of NSBs, formed by $z = z$, that do not merge by $z = 0$. In our fiducial case, about 40% of the NSBs that do not contribute to r-process enrichment by $z = 0$ is because of the delay time they experience before merging. The solid purple line shows the sum of the two cumulative solid blue and solid green lines and therefore represents the overall cumulative fraction of all NSBs that do not contribute to r-process enrichment as a function of redshift.

In Figure 2, we compare the overall cumulative fraction of not-contributing NSBs with different assumptions regarding the coalescence timescale of the binaries. The red dashed and green dot-dashed lines show the cumulative fraction of NSBs that do not contribute to r-process enrichment by $z = 0$ assuming a constant t_{coal} of 30 and 100 Myr, respectively. The short coalescence timescales in the case of constant t_{coal} leave no room for the NSBs to not merge by $z = 0$. Using a constant timescale instead of a DTD for the coalescence times of NSMs decreases the total fraction of non-contributing NSBs from $\sim 40\%$ to $\sim 30\%$ for $t_{\text{coal}} = 100$ Myr, and to $\sim 15\%$ in the case of $t_{\text{coal}} = 30$ Myr.

We also changed the minimum timescale for merging in DTD assumption from 10 Myr to 100 Myr and just observed a difference of 10% in the total fraction of the NSBs compared to the fiducial case. This is because longer timescale for merging results in both an increase in the fraction of NSBs that do not have time to merge and also let the NSBs to travel further out inside the virialized halo, an effect that is in place since $z \sim 1.5$.

In Figure 3 we compare the assumption we put for the radius beyond which a NSM do not contribute to r-process enrichment. We compare two cases where $R_{\text{enc}} = 2$ and $4 \times R_{\text{eff}}$ and see that considering $f_{\text{enc}} = 4$ leads to 25% more NSBs contributing to r-process enrichment (blue solid lines). The effect is more pronounced when using higher median natal kick velocities. With a low median velocity (red dashed lines), NSBs at low redshift eventually become unable to travel beyond the defined enclosed radius, regardless of their coalescence times. In that case, by increasing f_{enc} , the cumulative fraction of non-contributing NSBs ap-

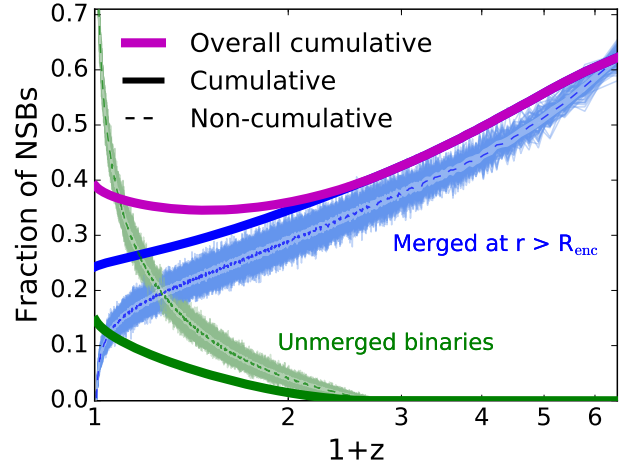


Figure 1. Fraction of NSBs that do *not* contribute to r-process enrichment. The blue dashed line represents the fraction of NSBs formed at redshift z that do not contribute to r-process enrichment at the time of their merging because this occurs far from the galaxy ($r > 2R_{\text{eff}}$). The green dashed line shows the fraction of NSBs formed at redshift z that do not merge by $z = 0$ because of the delay in their coalescence. Shaded light blue and light green regions show the results of 100 simulations. The smaller white shaded areas wrapping the dashed lines represent the 68% confidence interval. The solid lines show the cumulative results, meaning the fraction of all the NSBs formed by redshift z have not contributed to r-process enrichment either because they merge outside a multitude of the galaxy’s effective radius (solid blue) or have not merged yet by redshift z (solid green). The purple solid line shows the overall cumulative non-contributing fraction of NSBs by redshift z which is the sum of the green and blue solid lines.

proaches 15%, the fraction of NSBs that do not have time to merge by $z = 0$.

4 DISCUSSION

This work consists of a first step towards a more complex and realistic approach we will present in an upcoming work. We did not consider a disc shape for the galaxy at low redshifts when tracing the trajectory of the binary. Depending on the natal kick and coalescence timescale of a NSB, the NSM will have more chance to occur beyond the star-forming region if the binary system is kicked perpendicularly to the galactic plane. For the largest enclosing radius considered in this work ($4 R_{\text{eff}}$), the orientation of the kick relative to the galactic plane becomes less problematic. In addition, we assumed that all the trajectories originate from the center of the galaxy. A more realistic approach would be to spatially distribute the initial position of the binaries according to the stellar density profile, which could be done when accounting for the shape of the central galaxy.

Introducing a disc geometry in our work would also allow to account for the impact of binaries angular momentum on their trajectory. Depending on the angle between the natal kick velocity vector and that of its angular momentum, the effect of the natal kick will be different, which could modify the predicted fraction of non-contributing NSMs on r-process enrichment. One of our next improvements will be

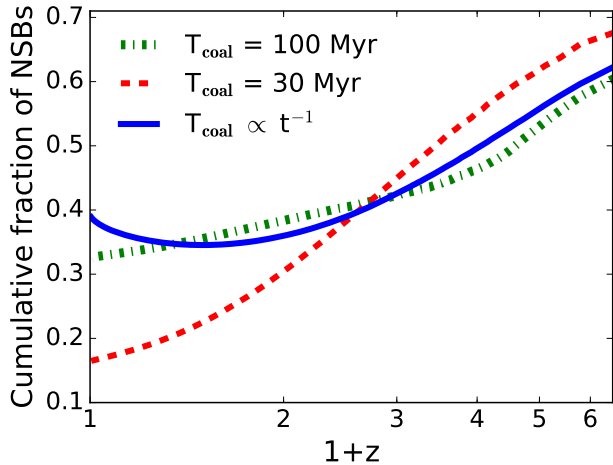


Figure 2. Impact of the delay-time distribution assumption of NSMs on the cumulated fraction of NSBs formed by redshift z , that do not contribute to *r*-process evolution as a function of redshift. Each line represents the median value of 100 simulations. The blue solid line shows the result of using a power-law delay-time distribution function with a minimum coalescence time of 30 Myr. The red dashed and green dot-dashed

lines are the result of using a constant coalescence timescale of 30 and 100 Myr, respectively, after which all NSMs occur in a simple stellar population. In these two last cases, no NSM is left unmerged by $z = 0$ because there is no NSM with long delay times.

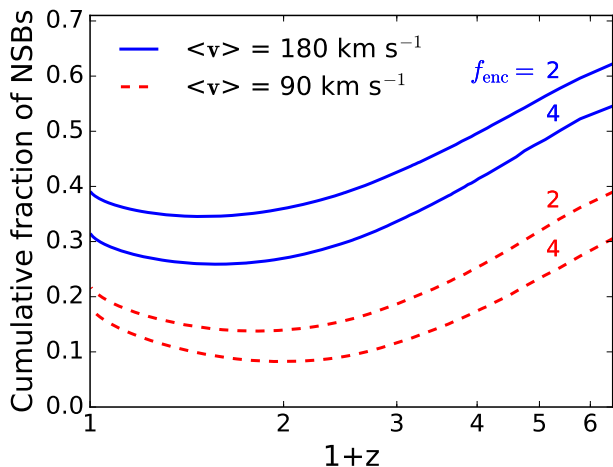


Figure 3. Impact of the enclosing radius on the cumulative fraction of NSBs that do not contribute to *r*-process enrichment by redshift z . Each line represents the median value of 100 simulations. Different lines represent different enclosing radius $R_{\text{enc}} = f_{\text{enc}} R_{\text{eff}}$, as indicated next to each line in the panel. Solid blue (dashed red) lines present the results when adopting a natal kick distribution with $\langle v \rangle = 180$ (90) km s^{-1} .

to follow the trajectory of NSBs in 3D instead of 1D and to account for their location within the disc along with the orientation of their kick with respect to the galactic plane when the disk potential is also taken into account.

Our fiducial model is based on the assumption that the natal kick PDF of NSBs follows an exponential distribution with an average velocity of $\langle v \rangle = 180 \text{ km s}^{-1}$ (see Sec-

tion 2.4). Fong & Berger (2013), however, derived lower velocities in the range of $20\text{--}140 \text{ km s}^{-1}$ with a median value around 60 km s^{-1} . In addition, Beniamini & Piran (2016) showed that the natal kick distribution can be bimodal with a low-velocity component below $\sim 30 \text{ km s}^{-1}$. Following Behroozi et al. (2014), we tested an exponential velocity PDF with $\langle v \rangle = 90 \text{ km s}^{-1}$ to represent Fong & Berger (2013) findings. As shown in Figure 3, reducing $\langle v \rangle$ by a factor of 2 reduces the fraction of non-contributing NSBs by a factor between 1.5 and 2, which demonstrates that the choice of the natal kick PDF has a non-negligible impact on our results.

The rates of NSMs derived from pulsar luminosity distribution (Kalogera et al. 2004; Abadie et al. 2010) and from gravitational wave measurements (Advanced LIGO, Abbott et al. 2016) are uncertain by about 3 orders of magnitude. A similar range is predicted by population synthesis models (Dominik et al. 2012). However, as we do not vary the number of NSMs (per units of stellar mass formed) throughout our calculations and only calculate the *fraction* of non-contributing NSBs, the total number of NSMs formed in our simulation does not impact our results and therefore these large uncertainties do not affect the quantities derived in this paper. That said, those uncertainties will affect the contribution of NSMs on the evolution of *r*-process in the MW, as the level of enrichment is directly proportional to the number of enriching sources.

5 CONCLUSIONS

We presented a parametrized approach to quantify the impact of NSB natal kicks on *r*-process enrichment of a MW-like galaxy by NSMs. The progenitor halo mass is parametrized to be consistent with the results of N-body simulations. The SFH is adopted from an abundance matching technique and the size evolution of the galaxy is taken to be in agreement with observations. NSMs are born with a natal kick and delay time for merging and we follow their trajectory in radial direction inside their host halo potential. If a NSB merges beyond twice the galaxy’s effective radius, we consider that binary to not contribute to *r*-process enrichment.

Given the caveats stated in Section 4 and the absence of gas recycling in our model, we predict that up to 40% of all the NSBs formed in the entire star formation history of a MW-like galaxy do not contribute to *r*-process enrichment either because they merge well beyond the galaxy’s effective radius at a given redshift or because of the delay they experience in merging. About 15% of all NSBs are predicted to be free floating in the MW halo. This result is based on a power law DTD motivated by Dominik et al. (2012) and an exponential natal kick velocity suggested by Behroozi et al. (2014) with an average velocity of 180 km s^{-1} .

Implementing the natal kicks together with delay-time distributions in hydrodynamical simulations of *r*-process enrichment such as those carried out by van de Voort et al. (2015), Hirai et al. (2015), and Safarzadeh & Scannapieco (in prep) would be the closest simulation to reality, but it is not clear how futuristic this approach would be in order to arrive at a significant statistics. Our results in this paper is a first order estimate on the impact of the natal kicks

and provides correction factors for r-process enrichment as a function of redshift for a MW type halo, though the corrections would be more in agreement with hydro simulations at higher ($z > 1$) redshifts as the geometry of a disc is not taken into account in this work.

In a forthcoming paper, we plan to use the NSM delay-time and natal kick PDFs predicted by population synthesis models (e.g., Fryer et al. 1998; Belczynski et al. 2002; Dominik et al. 2012; Belczynski et al. 2016). This will enable to account for the variation with metallicity (redshift) of the total number of NSMs per unit of stellar mass formed as well as the variation of the shape of the PDFs. Such variations are rarely included in galactic chemical evolution simulations (but see Mennekens & Vanbeveren 2016), although they can significantly modify the chemical evolution trends (Côté et al. 2017). This complementary study will provide insights into the impact of using different modeling assumptions for NSMs.

6 ACKNOWLEDGEMENTS

We are thankful to the anonymous referee for their constructive comments. We are also thankful to Chris Fryer, Chris Belczynski, and Evan Scannapieco for useful discussions. MS and BC are supported by the National Science Foundation (USA) under Grant No. PHY-1430152 (JINA Center for the Evolution of the Elements).

REFERENCES

- Abadie J., et al., 2010, *Classical and Quantum Gravity*, **27**, 173001
- Abbott B. P., et al., 2016, *ApJ*, **832**, L21
- Argast D., Samland M., Thielemann F. K., Qian Y. Z., 2004, *Astronomy & Astrophysics*, **416**, 997
- Arzoumanian Z., Chernoff D. F., Cordes J. M., 2002, *ApJ*, **568**, 289
- Behroozi P. S., Wechsler R. H., Conroy C., 2013, *ApJ*, **770**, 57
- Behroozi P. S., Ramirez-Ruiz E., Fryer C. L., 2014, *ApJ*, **792**, 123
- Belczynski K., Bulik T., 1999, *A&A*, **346**, 91
- Belczynski K., Kalogera V., Bulik T., 2002, *ApJ*, **572**, 407
- Belczynski K., Perna R., Bulik T., Kalogera V., Ivanova N., Lamb D. Q., 2006, *ApJ*, **648**, 1110
- Belczynski K., Repetto S., Holz D. E., O’Shaughnessy R., Bulik T., Berti E., Fryer C., Dominik M., 2016, *ApJ*, **819**, 108
- Beniamini P., Piran T., 2016, *MNRAS*, **456**, 4089
- Beniamini P., Hotokozaka K., Piran T., 2016, *The Astrophysical Journal Letters*, **829**, L13
- Berger E., 2010, *The Astrophysical Journal*, **722**, 1946
- Bloom J. S., Sigurdsson S., Pols O. R., 1999, *MNRAS*, **305**, 763
- Bramante J., Linden T., 2016, *The Astrophysical Journal*, **826**, 57
- Brown T. M., et al., 2012, *The Astrophysical Journal Letters*, **753**, L21
- Cescutti G., Romano D., Matteucci F., Chiappini C., Hirschi R., 2015, *A&A*, **577**, A139
- Côté B., Belczynski K., Fryer C. L., Ritter C., Paul A., Wehmeyer B., O’Shea B. W., 2017, *ApJ*, **836**, 230
- Cowan J. J., Thielemann F.-K., Truran J. W., 1991, *Physics Reports*, **208**, 267
- Dominik M., Belczynski K., Fryer C., Holz D. E., Berti E., Bulik T., Mandel I., O’Shaughnessy R., 2012, *ApJ*, **759**, 52
- Dutton A. A., Macciò A. V., 2014, *MNRAS*, **441**, 3359
- Fischer T., Martínez-Pinedo G., Hempel M., Liebendörfer M., 2012, *Physical Review D*, **85**, 857
- Fong W., Berger E., 2013, *ApJ*, **776**, 18
- Frebel A., Bromm V., 2012, *The Astrophysical Journal*, **759**, 115
- Fryer C., Burrows A., Benz W., 1998, *ApJ*, **496**, 333
- Fryer C. L., Woosley S. E., Hartmann D. H., 1999, *ApJ*, **526**, 152
- Goriely S., Bauswein A., Janka H.-T., 2011, *The Astrophysical Journal Letters*, **738**, L32
- Goriely S., Bauswein A., Just O., Pllumbi E., Janka H. T., 2015, *Monthly Notices of the Royal Astronomical Society*, **452**, 3894
- Hansen B. M. S., Phinney E. S., 1997, *MNRAS*, **291**, 569
- Hirai Y., Ishimaru Y., Saitoh T. R., Fujii M. S., Hidaka J., Kajino T., 2015, *ApJ*, **814**, 41
- Hirai Y., Ishimaru Y., Saitoh T. R., Fujii M. S., Hidaka J., Kajino T., 2017, *MNRAS*, **466**, 2474
- Hobbs G., Lorimer D. R., Lyne A. G., Kramer M., 2005, *MNRAS*, **360**, 974
- Ishimaru Y., Wanajo S., Prantzos N., 2015, *ApJ*, **804**, L35
- Kalogera V., Lorimer D. R., 2000, *ApJ*, **530**, 890
- Kalogera V., et al., 2004, *ApJ*, **614**, L137
- Kelley L. Z., Ramirez-Ruiz E., Zemp M., Diemand J., Mandel I., 2010, *The Astrophysical Journal Letters*, **725**, L91
- Klypin A. A., Trujillo-Gomez S., Primack J., 2011, *ApJ*, **740**, 102
- Komiya Y., Shigeyama T., 2016, *ApJ*, **830**, 76
- Korobkin O., Rosswog S., Arcones A., Winteler C., 2012, *Monthly Notices of the Royal Astronomical Society*, **426**, 1940
- Kravtsov A. V., 2013, *ApJ*, **764**, L31
- Lorimer D. R., 2008, *Living Reviews in Relativity*, **11**
- Martínez-Pinedo G., Fischer T., Lohs A., Huther L., 2012, *Physical Review Letters*, **109**, 251104
- Matteucci F., Romano D., Arcones A., Korobkin O., Rosswog S., 2014, *MNRAS*, **438**, 2177
- Mennekens N., Vanbeveren D., 2016, *A&A*, **589**, A64
- Moster B. P., Naab T., White S. D. M., 2013, *MNRAS*, **428**, 3121
- Nishimura N., Takiwaki T., Thielemann F.-K., 2015, *The Astrophysical Journal*, **810**, 109
- Oechslin R., Rosswog S., Thielemann F.-K., 2002, *Physical Review D*, **65**, 103005
- Piran T., Nakar E., Rosswog S., 2013, *Monthly Notices of the Royal Astronomical Society*, **430**, 2121
- Planck Collaboration et al., 2016, *A&A*, **594**, A13
- Roberts L. F., Reddy S., Shen G., 2012, *Physical Review C*, **86**, 065803
- Rosswog S., Liebendörfer M., Thielemann F. K., Davies M. B., Benz W., Piran T., 1999, *Astronomy & Astrophysics*, **341**, 499
- Rosswog S., Davies M. B., Thielemann F. K., Piran T., 2000, *MNRAS*, **360**, 171
- Shappee B. J., Thompson T. A., 2013, *The Astrophysical Journal*, **766**, 64
- Shen S., Cooke R. J., Ramirez-Ruiz E., Madau P., Mayer L., Guedes J., 2015, *The Astrophysical Journal*, **807**, 115
- Vargas L. C., Geha M., Kirby E. N., Simon J. D., 2013, *The Astrophysical Journal*, **767**, 134
- Wanajo S., 2013, *The Astrophysical Journal*, **770**, L22
- Wanajo S., Janka H.-T., Müller B., 2010, *The Astrophysical Journal Letters*, **726**, L15
- Wanajo S., Sekiguchi Y., Nishimura N., Kiuchi K., Kyutoku K., Shibata M., 2014, *The Astrophysical Journal Letters*, **789**, L39
- Wang W., Han J., Cooper A. P., Cole S., Frenk C., Lowing B., 2015, *MNRAS*, **453**, 377
- Wehmeyer B., Pignatari M., Thielemann F.-K., 2015, *MNRAS*, **452**, 1970
- Winteler C., Käppeli R., Perego A., Arcones A., Vasset N., Nishimura N., Liebendörfer M., Thielemann F. K., 2012, *The Astrophysical Journal Letters*, **750**, L22
- Woosley S. E., Wilson J. R., Mathews G. J., Hoffman R. D., Meyer B. S., 1994, *Astrophysical Journal*, **433**, 229

Zemp M., Ramirez-Ruiz E., Diemand J., 2009, *The Astrophysical Journal*, 705, L186
van de Voort F., Quataert E., Hopkins P. F., Kereš D., Faucher-Giguère C.-A., 2015, *Monthly Notices of the Royal Astronomical Society*, 447, 140
van der Wel A., et al., 2014, *ApJ*, 788, 28

This paper has been typeset from a $\text{\TeX}/\text{\LaTeX}$ file prepared by the author.